J. Phys. Chem. 1983, 87, 3983-3988

Dimer Cation Formation in Anionic Microemulsion Media. Duroquinone-Sensitized Photooxidation of 2,6-Dimethylnaphthalene and Tetrathiafulvalene

Carole K. Grätzel,* Akira Kira, Marie Jirousek, and Michael Grätzel

Institut de Chimie Physique, Ecole Polytechnique Fédérale, CH-1015 Lausanne, Switzerland

(Received: November 1, 1982; In Final Form: March 16, 1983)

Flash photolysis studies using a ruby laser ($\lambda = 347$ nm, doubled line) were performed on the systems duroquinone (DQ)/2,6-dimethylnaphthalene (DMN) and DQ/tetrathiafulvalene (TTF) principally in sodium hexadecyl sulfate (SCS) microemulsion media. Electron transfer from both DMN and TTF to triplet duroquinone with efficient charge separation to produce the product cations and anion was observed in these media. Identical experiments performed in homogeneous media demonstrated electron transfer but with less efficient charge separation and consequently lower product ion yields. Dimer cation formation of both DMN and TTF, i.e., $(DMN)_2^+$ and $(TTF)_2^+$, in the anionic microemulsion media was readily detected. The formation of $(TTF)_2^+$ was reverified by pulse radiolysis experiments. Although tetrathiafulvalene stacks easily in organic conducting salts and thus should have no difficulty in obtaining the supposed sandwichlike configuration of the dimer, no previous reports announce its detection. Dimer cation formation of aromatic compounds in microemulsion media is unique in itself since the majority of previous studies of this type involved γ irradiation of substrate solubilized in glassy alkane matrices at low temperatures (77 K). The dimer formation constant for DMN was evaluated graphically as $K = 4.76 \times 10^2$.

Introduction

Quinoid compounds have been extensively studied in the past, one important aspect being their biological implications in the electron-transport system of photosynthesis. Here alkylated quinones serve as electron acceptors, and the doubly reduced species, the hydroquinones, as electron donors linking PSI and PSII through their presence in "plastiquinone pools" within the chloroplast membranes.[1-3] The radiation-induced reduction of many substituted quinones, e.g., methylated *p*-benzoquinones, including duroquinone (tetramethylbenzoquinone), toluquinone, xyloquinone, naphthoquinone, and anthraquinone have been thoroughly investigated by means of steady-state[4] and flash[5-8] photolysis and the pulse radiolysis technique.[9,10] Consequently, the absorption wavelengths and their respective extinction coefficients corresponding to the duroquinone triplet (DQ^T, $\lambda_{max} \simeq 490$ nm) and its semiquinone radical ($DQH\cdot$, $\lambda_{max} \simeq 420$ nm) have all been positively identified. Complementary studies on the photooxidation of hydroquinones have also been pursued.[2,3] The majority of these studies have been performed in homogeneous solutions such as 2-propanol, acetone, hexane, liquid paraffin, and water/organic mixtures, etc. However, Grätzel et al.[11-13] and other groups[14-17] found that ion product formation and stabilization were enhanced in micellar solution. Fairly recently, Kiwi and Grätzel[18] extended these studies to the electron transfer from diphenylamine to duroquinone in anionic microemulsion solution and found that the solubility of reactants was enhanced relative to the sister micelles. They found that efficient charge separation also occurred in these media. Interestingly, they also witnessed aggregate (dimer) cation formation induced by the high local concentration of reactants within the microemulsion droplets.

The experiments presented herein continue in this direction using 2,6-dimethylnaphthalene (DMN) and tetrathiafulvalene (TTF) as electron donors cosolubilized with duroquinone (electron acceptor) in sodium hexadecyl sulfate (SCS) microemulsion media. Experiments were also performed in homogeneous solution for comparison. Since SCS is an anionic surfactant, the DQ^- formed should be ejected quickly from the hydrocarbon interior into the aqueous phase ($DQH\cdot$), while the oxidation products (cations) of DMN and TTF should remain solubilized in the lipoidic microdroplet core.

Numerous investigations have followed the γ-irradiation formation of cation radicals of aromatic hydrocarbons,[19,40,41] generally in glassy (alkane or freon) matrices at low temperatures (~77 K).[20-22] In those studies, the dimer cations of these species can be formed either by the diffusion-controlled bimolecular reactions of a monomer cation with a neutral (relaxed dimer cation) or through the trapping

---

(1) J. Amesz, *Biochim. Biophys. Acta*, **301**, 35 (1973).

(2) J. R. Darwent, K. Kalyanasundaram, and G. Porter, *Proc. R. Soc. London, Ser. A*, **373**, 179 (1980).

(3) J. R. Darwent and K. Kalyanasundaram, *J. Chem. Soc., Faraday Trans. 2*, **77**, 373 (1981).

(4) J. Nafisi-Movaghar and F. Wilkinson, *Trans. Faraday Soc.*, **66**, 2257 (1970).

(5) N. K. Bridge and G. Porter, *Proc. R. Soc. London, Ser. A*, **244**, 259 (1958).

(6) F. Wilkinson, G. M. Seddon, and K. Tickle, *Ber. Bunsenges. Phys. Chem.*, **72**, 315 (1968).

(7) J. Nafisi-Movaghar and F. Wilkinson, *Trans. Faraday Soc.*, **66**, 2268 (1970).

(8) D. R. Kemp and G. Porter, *Proc. R. Soc. London, Ser. A.*, **326**, 117 (1971).

(9) E. J. Land, *Trans. Faraday Soc.*, **65**, 2815 (1969).

(10) K. B. Patel and R. L. Willson, *J. Chem. Soc., Faraday Trans. 1*, **69**, 814 (1973).

(11) C. Wolff and M. Grätzel, *Chem. Phys. Lett.*, **52**, 542 (1977).

(12) R. Scheerer and M. Grätzel, *J. Am. Chem. Soc.*, **99**, 865 (1977).

(13) S. A. Alkaitis, M. Grätzel, and A. Henglein, *Ber. Bunsenges. Phys. Chem.*, **79**, 541 (1975).

(14) K. Kano and T. Matsuo, *Bull. Chem. Soc. Jpn.*, 47, 2836 (1974).

(15) K. Kano, Y. Takada, and T. Matsuo, *Bull. Chem. Soc. Jpn.*, **48**, 3215 (1975).

(16) H. Inoue and M. Hida, *Chem. Lett.*, 107 (1979).

(17) K. Kano, K. Takuma, T. Ikeda, D. Nakajima, Y. Tsutsui, and T. Matsuo, *Photochem. Photobiol.*, **27**, 695 (1978).

(18) J. Kiwi and M. Grätzel, *J. Am. Chem. Soc.*, **100**, 6314 (1978).

(19) A. Kira, S. Arai, and M. Imamura, *J. Chem. Phys.*, **54**, 4890 (1971).

(20) T. Shida and S. Awata, *J. Am. Chem. Soc.*, **95**, 3473 (1973).

(21) T. Shida, Y. Nosaka, and T. Kato, *J. Phys. Chem.*, **82**, 695 (1978).

(22) A. Kira and M. Imamura, *J. Phys. Chem.*, **83**, 2267 (1979).

0022-3654/83/2087-3983\$01.50/0

of positive holes migrating in the matrix by already existing neutral dimer molecules (unrelaxed dimer cation). The dynamic formation and behavior of these dimer cation radicals is thus followed by observing the optical spectra changes upon controlled warming of the alkane (Freon) matrix. Especially well-known are the spectra of the naphthalene cation and dimer cation.[22-24] (ESR studies of chemically oxidized ($SbCl_5$) aromatics such as naphthalene and anthracene and their substituted derivatives have also proven the existence of their monomer and dimer cations.[25-27]) These studies may be, however, often severely limited by the constraint to warm the matrices in order to follow the dimer cations' reaction dynamics.

A microemulsion droplet's core in effect acts as a softened matrix since it is a localized viscous hydrocarbon site where movement is somewhat restrained. However, it has the advantage in that one is not obliged to warm it in order to study the dynamical features of the dimer cation radicals' formation and decay. Thus, spectral interference from matrix cracking is avoided. Utilization of microemulsion media also leads to facile observation of the dimer cation's formation equilibrium by varying the concentration of aromatic compound solubilized in the lipoidic microemulsion core. In this study, ready oxidation of DMN to DMN^+ by triplet DQ (laser photoexcited) occurs. The DMN^+ thus produced attacks a neutral DMN molecule to form its dimer cation, $(DMN)_2^+$.

Tetrathiafulvalene has been the subject of many studies, primarily synthetic, due to its conducting properties in "organic metals" such as $TCNQ^-$–TTF^+.[28-31] This compound was more recently utilized as a photoelectron donor in an experimental investigation of electron-transfer reactions using zinc tetrakis(*p*-sulfonatophenyl)porphyrin and $Ru(bpy)_3^{2+}$ as sensitizers in cationic micellar and microemulsion media.[32] This work includes a complementary study on TTF's electron-transfer properties in anionic microemulsion media using DQ as a sensitizer. The previously unreported dimer cation formation of tetrathiafulvalene is witnessed.

Experimental Section

Materials. Duroquinone (Aldrich, 97%) was sublimed before utilization to form needlelike bright yellow crystals. 2,6-Dimethylnaphthalene (Fluka purum) and tetrathiafulvalene (Fluka puriss, 99%) were used as supplied with no further purification. The sodium hexadecyl (cetyl) sulfate (Merck) used in the surfactant assemblies was also used as supplied. The 1-pentanol used in the preparation of the microemulsions was distilled once before utilization. The hexadecane (Fluka purum) was used as the oil component of the microemulsion without purification. Cetyltrioxyethylene sulfate sodium salt (CTOES) from Henkel, Cie was used without purification for the preparation of the micelles utilized in the pulse radiolysis experiments. All of the water used in the preparation of the microemulsion and micellar solutions was distilled once from alkaline permanganate and subsequently twice from a quartz still.

Preparation of Organized Assembly Solutions. The high water (75.6%) content SCS microemulsions were prepared as follows: 7.9% SCS was dissolved in 3.2% hexadecane and 13.4% 1-pentanol and then diluted with 75.6% water (all percentages by weight). For the preparation of the microemulsions with solubilized components, concentrated stock solutions of duroquinone, 2,6-dimethylnaphthalene, and tetrathiafulvalene were prepared in 1-pentanol, and for TTF also in hexadecane, and then degassed. Dilutions of the pure components by these concentrated stock solutions appropriate to the desired solubilizate concentration were made. All solutions were degassed both prior to and after addition of the solubilizates for a total of approximately 30 min to ensure oxygen-free solutions for the laser photolysis experiments. For the pulse radiolysis experiments, tetrathiafulvalene was solubilized (5×10^{-4} M) in the CTOES micelles (5×10^{-3} M) 0.1 M in NaBr by slow injection (10 μL per aliquot) of a concentrated solution of tetrathiafulvalene in tetrahydrofuran (THF). The solution was then mildly heated and degassed by argon to ensure the evaporation of trace amounts of THF. The solution was subsequently N_2O saturated by bubbling for ~10 min. Light-sensitive solutes such as tetrathiafulvalene were protected from stray ambient light to avoid degradation. The concentrations were reverified by absorption spectroscopy.

Apparatus. A Q-switched J.K.-2000 Ruby laser (doubled line, 347.1 nm) was used as the excitation source in all of the flash photolysis experiments. The pulse had a duration of 15 ns and an energy between 30 and 300 mJ. A 400-W XBO xenon lamp served as the light source in a detection system already described.[33] Transient spectra were recorded by using the fast kinetic spectroscopy technique. Verification of all concentrations was accomplished with a Perkin-Elmer Hitachi 340 vis–UV absorption spectrometer.

Pulse radiolysis experiments were performed with a 3-MeV (High Voltage Co.) Van de Graaf using a 40-ns pulse width with a current of 200 mA. Transients were detected by kinetic spectroscopy as previously described for photolysis experiments.[33]

Results and Discussion

The laser photolysis experiments were all performed either in anionic microemulsion media (SCS) or in homogeneous (acetonitrile) solution. In the microemulsion system both substrates (DMN (or TTF) and DQ) were solubilized in the microemulsion droplets' interior. Flash photolysis by the doubled ruby laser line (λ = 347 nm) yields the triplet state of duroquinone which participates in a charge-transfer reaction with 2,6-dimethylnaphthalene to form its anion (DQ^-) and the cation of DMN according to eq 1. The DQ^- thus formed should be immediately

$$DQ^T + DMN \rightarrow DMN^+ + DQ^- \qquad (1)$$

ejected (within a few microseconds) from the interior of the microemulsion into the aqueous phase due to the negative potential within the lipoidic core of the microemulsion. A Stern–Volmer plot gives the quenching constant of the DQ triplet as $k_q \simeq 3 \times 10^7$ M^{-1} s^{-1} ± 6%, as exhibited in Figure 1 (a decay curve (λ = 490 nm) typical for the triplet quenching at 12 mM DMN is depicted in the insert; one notes a slow decaying tail attributed to the monomer cation.)[34] This reaction occurs readily as is

---

(23) A. Kira, M. Imamura, and T. Shida, *J. Phys. Chem.*, **80**, 1445 (1976).

(24) B. Badger and R. Brocklehurst, *Trans. Faraday Soc.*, **65**, 2588 (1969).

(25) S. C. Lewis and L. S. Singer, *J. Chem. Phys.*, **43**, 2712 (1965).

(26) O. W. Howarth and G. K. Fraenkel, *J. Chem. Phys.*, **52**, 6258 (1970).

(27) B. Badger, B. Brocklehurst, and R. D. Russell, *Chem. Phys. Lett.*, **1**, 122 (1967).

(28) J. Ferraris, D. O. Cowan, V. Walatka, Jr., and J. H. Perlstein, *J. Am. Chem. Soc.*, **95**, 948 (1973).

(29) J. P. Ferraris, T. O. Poehler, A. N. Block, and D. O. Cowan, *Tetrahedron Lett.*, **27**, 2553 (1973).

(30) J. H. Perlstein, *Angew. Chem., Int. Ed. Engl.*, **16**, 519 (1977).

(31) J. B. Torrance, *Acc. Chem. Res.*, **12**, 79 (1979).

(32) C. K. Grätzel and M. Grätzel, *J. Phys. Chem.*, **86**, 2710 (1982).

(33) G. Rothenberger, P. P. Infelta, and M. Grätzel, *J. Phys. Chem.*, **85**, 1850 (1981).

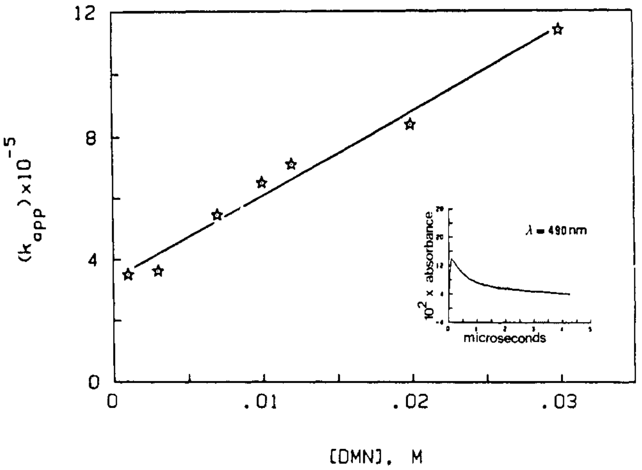

Figure 1. Stern-Volmer determination of the quenching constant for DQ^T, $k \sim 3 \times 10^7$ M^{-1} s; insert: DQ triplet decay (λ = 490 nm) at 12 × 10^{-3} M DMN.

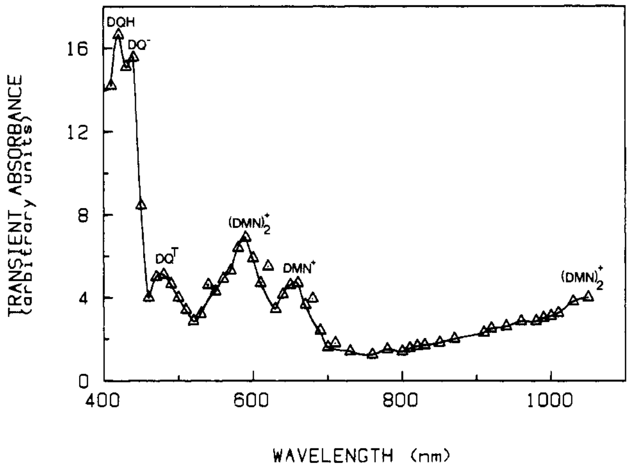

Figure 2. Difference spectrum taken immediately after laser excitation (λ = 347 nm) of DQ (10^{-3} M) and DMN (20 × 10^{-3} M) in SCS microemulsion media.

upheld by the difference spectrum of Figure 2 taken immediately after the laser pulse. Peaks at $\lambda \simeq 490$ nm ($\epsilon_{490} = 4700$ M^{-1} cm^{-1} in cyclohexane, 9800 M^{-1} cm^{-1} in benzene), λ = 660 nm, and λ = 440 nm ($\epsilon = 7600$ M^{-1} cm^{-1} in aqueous 2-propanol (1 M) and acetone (1 M))[10] correspond to DQ^T, DMN^+ (monomer cation), and DQ^-, respectively. Since the pH of the microemulsion medium is ~7, one expects a fast protonation of the duroquinone anion to form the durosemiquinone radical, DQH, according to eq 2.

$$DQ^- + H^+ \rightleftarrows DQH \qquad (2)$$

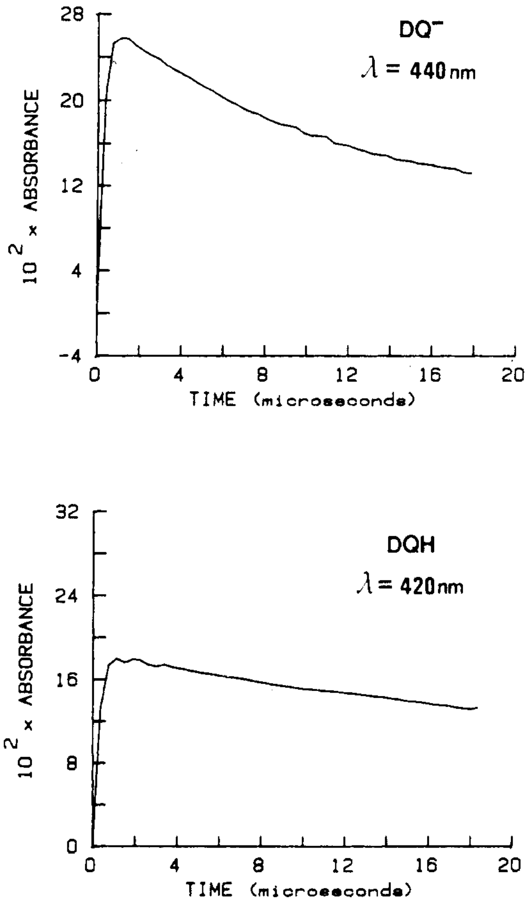

Figure 3. Laser absorption decay of DQ^- (λ = 440 nm) and DQH (λ = 420 nm) in SCS microemulsion media ([DQ] = 10^{-3} M, [DMN] = 15 × 10^{-3} M).

The dissociation constant of DQH in water has been measured as (8 ± 2) × 10^{-6} M.[37] This species has an absorption which maximizes at $\lambda \simeq 420$ nm ($\epsilon = 4700$ M^{-1} cm^{-1} in aqueous 2-propanol (1 M) and acetone (1 M))[10] (cf. Figure 2). The durosemiquinone radical can decay through dismutation to form duroquinone and durohydroquinone (eq 3).

$$2DQH \rightarrow DQ + DQH_2 \qquad (3)$$

The second-order rate constant for disappearance of DQH was measured as $k_2 \simeq 5.5 \times 10^8$ M^{-1} s^{-1} ± 3.2%. The anion may also disappear via dismutation according to reaction 4 after which rapid protonation of the dianion takes place

$$2DQ^- \rightarrow DQ + DQ^{2-} \qquad (4)$$

to form durohydroquinone

$$DQ^{2-} + 2H^+ \rightleftarrows DQH_2 \qquad (5)$$

The kinetics of the duroquinone anion (DQ^-) decay appear to be a competition of two second-order processes, i.e., (1) the slower than diffusion-controlled (bimolecular) reencountering of a DQ^- ejected from a droplet and a dissolved DMN^+ (there is a voltage barrier to overcome for this back-reaction), and (2) the bimolecular dismutation of two duroquinone anions to form a neutral duroquinone molecule and a dianion (this reaction will be completely diffusion controlled), followed by the rapid protonation of the dianion to form durohydroquinone. There may indeed be some contribution to the DQ^- (λ = 440 nm) peak due to overlapping absorption of the tail from the DQH (λ = 420 nm) peak; however, this contribution was ignored since

---

(34) It was deemed more appropriate to apply homogeneous rate laws for the treatment of kinetic events occurring in microemulsion droplets. This argument is based on the fact that the microemulsion droplet is larger and its charge density at the interface is smaller than for a micelle. Thus, exchange of the excited acceptor molecules (DQ^T) between different assemblies (~2 μs) is faster than the time scale on which the electron-transfer events occur (tens of microseconds). Consequently, the conditions necessary for treatment of the kinetic events by the intramicellar model developed by Infelta et al.[35] are not fulfilled. Also, in a very complete work by Kozak et al.,[36] it is pointed out that "the differences between homogeneous kinetics and intramicellar kinetics may be expected to be a rather sensitive function of the length ratio a_0/r_0 (where a_0 is the radius of the reacting molecular species and r_0 the radius of the droplet in which the reactants are confined). We anticipate that the greatest differences in kinetics will be found when $r_0 \gtrsim a_0$ but that experimental differences will converge rapidly when $r_0 \gg a_0$" (as is the case for a majority of microemulsion droplets).

(35) M. Maestri, P. P. Infelta, and M. Grätzel, *J. Chem. Phys.*, **69**, 1522 (1978).

(36) M. D. Hatlee, J. J. Kozak, G. Rothenberger, P. P. Infelta, and M. Grätzel, *J. Phys. Chem.*, **84**, 1508 (1980).

(37) R. L. Willson, *Chem. Commun.*, 1249 (1971).

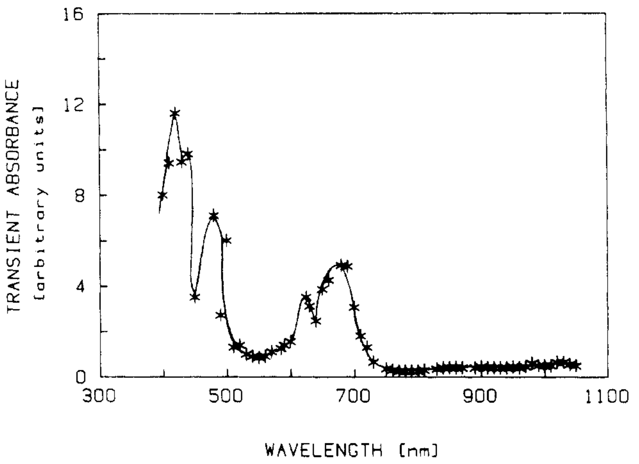

Figure 4. Difference spectrum taken immediately after laser excitation (λ = 347 nm) of DQ (10^{-3} M) and DMN (2×10^{-3} M) in SCS microemulsion media.

quantitative kinetic parameters were in any event impossible to discern due to the competitive second-order reactions explained above. The decay of the DQH would be superimposed at the end of the slower portion of the decay of DQ^- due to the different time scales for the two events. Photos taken after laser photolysis in Figure 3 show the kinetic characteristics of DQ^- and DQH.

The monomer cation of DMN, DMN^+ ($\lambda_{max} \simeq 680$ nm), can react further with neutral DMN molecules cosolubilized in the droplet's interior to form a dimer cation, $(DMN)_2^+$. The existence of this species is confirmed by a broad peak in the IR region ($\lambda \simeq 1050$ nm) of the difference spectrum of Figure 2 where DMN is present at the high concentration of 20 mM. The peak at $\lambda \simeq 580$ nm (there may also be a shoulder at ~550 nm) is the visible domain contribution of the dimeric cation.[27] At lower concentrations of DMN these dimeric species diminish as seen in the difference spectrum (Figure 4) taken immediately after laser excitation where the concentration of DMN was only 2 mM. Both the monomer and dimer cations' decays exhibit mixed-order kinetics due to a competition between the back-reaction of both the monomer and dimer cation with DQ^- (i.e., diffusion-controlled second-order reactions as explained previously for the decay of DQ^-) and pseudo-first-order reactions with nucleophilic species such as OH^- (see eq 6 and 7). Figure 5 exhibits the absorption decay curves for these two species at λ = 680 nm and λ = 1040 nm, respectively. By varying the concentration of DMN solubilized one has also the opportunity to determine the dimer formation constant, K, where $K = [d]/([DMN][m])$, [d] = concentration of dimer cation, and [m] = concentration of monomer cation. Since

$$\begin{tikzcd} DMN^+ + DMN \arrow[r, shift left, "k_3"] \arrow[d, "{[X^-]}"'] & (DMN)_2^+ \arrow[l, shift left, "k_4"] \arrow[d, "{[X^-]}"] \\ {[DMN^+-X^-]} & {[(DMN)_2^+-X^-]} \end{tikzcd}$$

(6)

(7)

$$OD^{1050} = l\epsilon_d^{1050}[d] \tag{8}$$

$$OD^{680} = l\{\epsilon_d^{680}[d] + \epsilon_m^{680}[m]\} \tag{9}$$

$$\frac{OD^{680}}{OD^{1050}} = \frac{\epsilon_d^{680}}{\epsilon_m^{150}}\left\{1 + \frac{\epsilon_m^{680}[m]}{\epsilon_d^{680}[d]}\right\} \tag{10}$$

Substituting $[m]/[d] = 1/(\alpha K[\overline{DMN}])$ where $\alpha[\overline{DMN}]$ = [DMN], and α is a partitioning fraction, since $[\overline{DMN}]$ is the bulk concentration used instead of the true concentration, [DMN], within the microemulsion droplet, one obtains

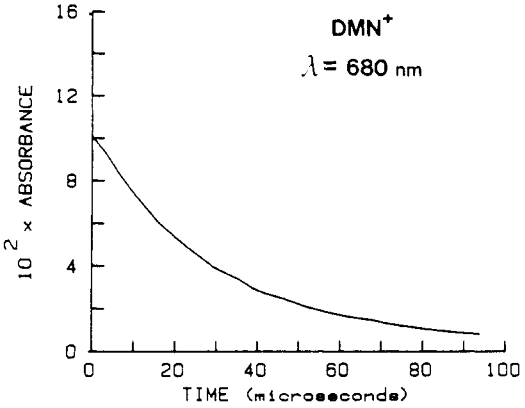

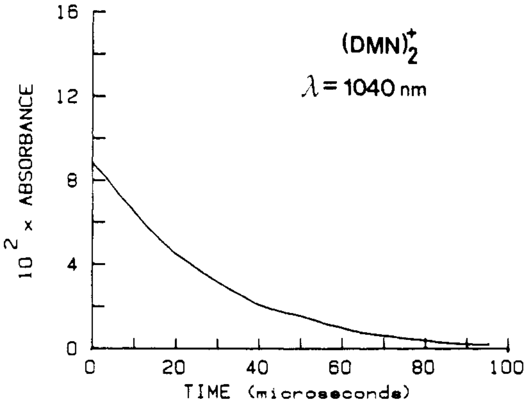

Figure 5. Laser absorption decay of DMN^+ (λ = 680 nm) and $(DMN)_2^+$ (λ = 1040 nm) in SCS microemulsion media ([DMN] = 20×10^{-3} M, [DQ] = 10^{-3} M).

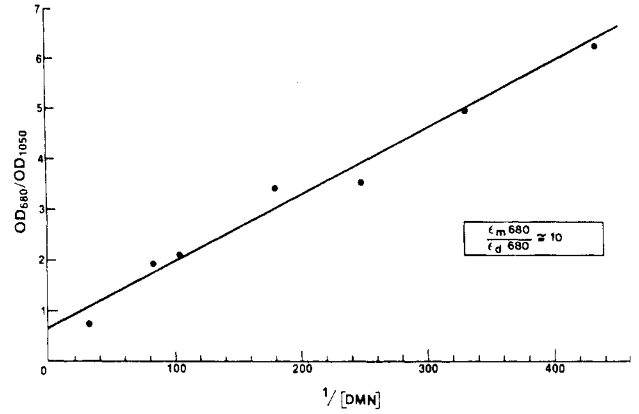

Figure 6. Graphical determination of dimer cation formation constant, $\bar{K} = [d^+]/([m^+][\overline{DMN}]) = 4.76 \times 10^2$, slope = $[\epsilon_m^{680}/(K\epsilon_d^{680})](\epsilon_d^{1050}/\epsilon_d^{680})$, intercept = $\epsilon_d^{680}/\epsilon_d^{1050}$.

$$\frac{OD^{680}}{OD^{1050}} = \frac{\epsilon_d^{680}}{\epsilon_d^{1050}}\left\{1 + \frac{\epsilon_m^{680}}{\bar{K}[\overline{DMN}]\epsilon_d^{680}}\right\} \tag{11}$$

Here $\alpha K = \bar{K}$, the observed formation constant. Thus, a plot of OD^{680}/OD^{1050} vs. $1/[\overline{DMN}]$ gives $\epsilon_d^{680}/\epsilon_d^{1050}$ as an intercept, and $\epsilon_m^{680}/(\bar{K}\epsilon_d^{680})$ as the slope divided by the intercept. Since the ratio of $\epsilon_m^{680}/\epsilon_d^{680}$ is known to be on the order of 10,[38] $\bar{K}$ can be evaluated. $\bar{K}$ evaluated

---

[38] A. Kira, unpublished results.

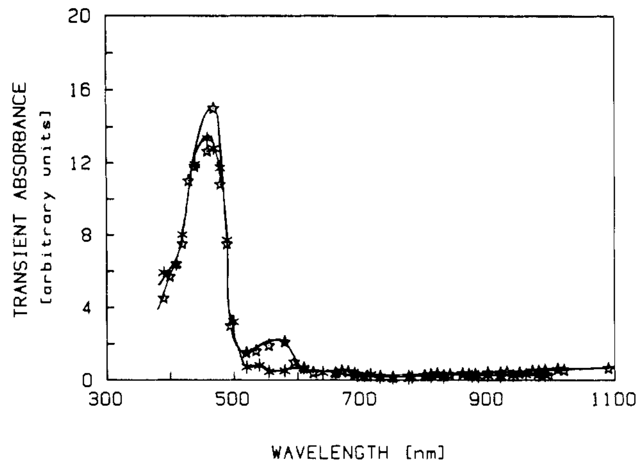

Figure 7. Difference spectrum taken immediately after laser excitation (λ = 347 nm) of DQ (10^{-3} M) and DMN (☆: 20 × 10^{-3} M; *: 2 × 10^{-3} M) in acetonitrile. The DQ triplet still contributes an absorption peak on the time scale of this spectrum.

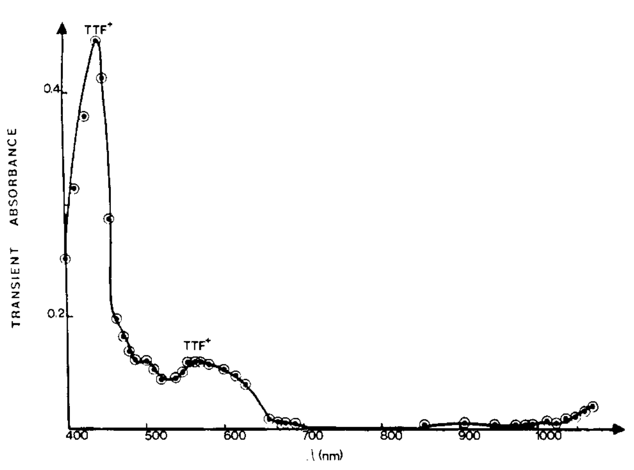

Figure 8. Difference spectrum taken immediately after laser excitation (λ = 347 nm) of TTF (5 × 10^{-3} M) and DQ (10^{-3} M) in a SCS microemulsion. $\lambda_{420-440}$: DQH, DQ^-, and TTF^+. λ_{580}: TTF^+, $\lambda_{\sim820}$: $(TTF)_2{}^+$.

graphically in this manner (see Figure 6) was found to be $\bar{K}$ = 4.8 × 10^2 ± 3.2%.

The charge-transfer reaction was accomplished in acetonitrile solution; however, the amount of product formed was greatly diminished. A small contribution for the dimer cation of DMN could be detected at $\lambda \simeq$ 580 nm when concentrations of DMN were as high as 20 mM; however, at 2 mM DMN only negligible amounts even of the monomer cation remained (see Figure 7). Consequently, it is readily seen that the microemulsion media enhance the electron-transfer reaction through physical separation of the charged species, thus inhibiting the back-reaction.

In the light-induced charge-transfer reaction of tetrathiafulvalene and duroquinone in SCS microemulsion media efficient product formation is also witnessed (eq 12).

$$DQ^T + TTF \rightarrow DQ^- + TTF^+ \qquad (12)$$

Accurate kinetic analysis for each of the species formed is rendered difficult due to spectral overlap; however, from the absorption maximum at $\lambda \sim$ 580 nm ($\epsilon_{TTF^+}^{580}$ = 5030 M^{-1} cm^{-1}, $\epsilon_{TTF^+}^{434}$ = 18600 M^{-1} cm^{-1} in acetonitrile),[39] and the broadening and loss of resolution of peaks at ~410–450 nm, one can identify the tetrathiafulvalene cation and the electron-transfer products of DQ. There is also an additional small peak at $\lambda \simeq$ 672 nm, and a broad hump in the IR similar to those seen in the DMN–DQ difference spectra (see difference spectrum of Figure 8). These peaks are attributed to a dimer cation of TTF (cf. 13).

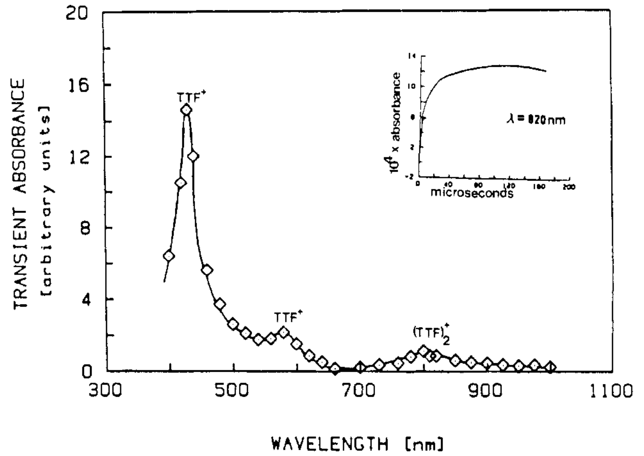

Figure 9. Difference spectrum taken (20-μs time scale after radiolysis (Van de Graaf) of TTF (5 × 10^{-4} M) in 0.1 M NaBr, N_2O-saturated CTOES micelles (5 × 10^{-3} M). $\lambda_{434,580}$: TTF^+, $\lambda_{\sim820}$: $(TTF)_2{}^+$. Insert: $(TTF)_2{}^+$ formation (λ = 820 nm).

$$TTF^+ + TTF \rightleftharpoons (TTF)_2{}^+ \qquad (13)$$

This hypothesis of dimer cation formation of TTF has been substantiated by pulse radiolysis experiments performed in CTOES micelles (5 × 10^{-3} M). These micellar solutions contain 0.1 M NaBr and are saturated by N_2O. The reaction sequence which occurs is, thus, as shown in eq 14–18. A broad peak in the IR between ~700 and 900

$$H_2O \rightarrow e^-(aq), H\cdot, \cdot OH \qquad (14)$$

$$N_2O + e^-(aq) \xrightarrow{H_2O} \cdot OH + N_2 + OH^- \qquad (15)$$

$$Br^- + \cdot OH \rightarrow Br\cdot + OH^- \qquad (16)$$

$$Br\cdot + Br^- \rightarrow Br_2{}^- \qquad (17)$$

$$Br_2{}^- + TTF \rightarrow TTF^+ + 2Br^- \qquad (18)$$

nm maximizing at $\lambda \simeq$ 820 nm is observed in the difference spectrum taken on this system (Figure 9). The dimer $(TTF)_2{}^+$ is seen to grow in on a time scale of 20 μs as depicted in the absorption curve at λ = 820 nm of the insert of this figure. Although dimer cation formation in a homogeneous medium (acetonitrile) has been suggested for the methylbenzo derivative of TTF[39]

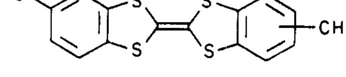

the dimer, $(TTF)_2{}^+$, has not previously been reported. The fact that our study indicates this formation is probably due to the high local concentrations present in the micellar and microemulsion entities. However, this occurrence should not be so surprising since the dimer cation is generally believed to maintain a sandwichlike configuration and TTF is known to stack very easily, even in a homogeneous medium.

The formation of the dimer cation would be in competition with nucleophilic attack (such as seen in eq 19) and dismutation reactions (eq 20 and 21) of TTF^+ which managed to escape to the aqueous phase.

$$TTF^+ + OH^- \rightarrow TTF\text{-}OH \qquad (19)$$

---

(39) S. Hünig, G. Kiesslich, H. Quast, and D. Scheutzow, *Justus Liebigs. Ann. Chem.*, 310 (1973).

(40) A. Kira, S. Arai, and M. Imamura *J. Phys. Chem.*, **76**, 1119 (1972).

(41) M. A. J. Rodgers, *J. Chem. Soc., Faraday Trans. 1*, **68**, 1278 (1972).

$$2\mathrm{TTF}^+ \rightarrow \mathrm{TTF} + \mathrm{TTF}^{2+} \quad (20)$$

$$\mathrm{TTF}^{2+} + 2\mathrm{OH}^- \rightarrow \mathrm{TTF{-}(OH)_2} \quad (21)$$

Conclusions

Dimer cations of large aromatic compounds such as naphthalene and its derivatives, anthracene, and pyrene have been demonstrated to exist. The majority of these studies were pursued in glassy matrices at low temperatures. Subsequent warming of the matrices led to detection of dimeric and even tetrameric species. Often this warming of the matrix caused cracking of the glass and was, thus, undesirable. Some of the dimers so formed were the product of hole capture of preexisting neutral dimer molecules and, consequently, in an excited-state configuration, i.e., "unrelaxed" dimer cations. The studies presented herein give the possibility of easily studying dimer cation formation resulting from the reaction of a monomer cation and a neutral molecule within the lipoidic core of the microemulsion droplet. The dimer cation, thus formed, is "relaxed" and can maintain its "normal" configuration (probably sandwichlike). Extremely interesting is the finding of a tetrathiafulvalene dimer cation. Although its formation should not be surprising due to the facility with which it stacks in organic conducting salts,[28] its spectral characteristics have not previously been reported. Microemulsions appear to be excellent media for examining such reactions as they give a relatively viscous environment which enhances agglomeration to form multimers without restricting the core solubilized molecules to a too great extent. The importance of the microemulsion droplets' ability to induce charge separation and to enhance substantial product ion formation should not be left unnoticed.

Registry No. 2,6-Dimethylnaphthalene, 581-42-0; tetrathiafulvalene, 31366-25-3; duroquinone, 527-17-3; sodium hexadecyl sulfate, 1120-01-0; 2,6-dimethylnaphthalene dimer cation, 38071-82-8; tetrathiafulvalene dimer cation, 70257-88-4.

Diffusion-Controlled Adsorption. Concentration Kinetics, Ideal Isotherms, and Some Applications

Harry L. Frisch

Department of Chemistry, State University of New York at Albany, Albany, New York 12222

and Karol J. Mysels*

Research Consulting, La Jolla, California 92037 *(Received: December 3, 1982)*

Changes of concentration $c(x,t)$ occurring in a quiescent solution, initially having a uniform concentration C_∞, during adsorption on a surface of arbitrary shape can be analyzed by using the method of reflections and superpositions. Diffusion to the surface, considered as a sink, yields one component of the total expression and diffusion from the surface, considered as a source, yields the other one. If the former is given by $C_\infty\psi(x,t)$, the latter becomes $\int_0^t(1 - \psi(x,t-\tau))\,\mathrm{d}c(0,\tau)$ where ψ is often well-known and $c(0,\tau)$ is the subsurface concentration at time τ. Each increment $\mathrm{d}c(0,\tau)$ is considered as a source acting for its lifetime $t - \tau$. The same kind of argument has previously yielded an expression relating $c(0,t)$ to the amount adsorbed and the adsorption isotherm. All these results involve integral equations, but, when the adsorption isotherm is ideal, Laplace transform methods can be used to obtain equations which can be solved explicitly for specific geometries. Application to the plane and the sphere gives such explicit solutions. One of these agrees with one pertinent specific solution found in the literature.

The kinetics of adsorption can be of intrinsic interest as providing clues to the molecular mechanism of this process or to the nature of the participating species; their understanding can help guide equilibrium adsorption studies; and they can be important in practical applications such as catalysis, flotation, detergency, or chromatography. Yet few theoretical models exist to help in designing or interpreting experiments. Even in one of the simplest cases, diffusion-controlled adsorption, the few equations available are presented as purely mathematical consequences of appropriate differential equations without providing insight into their physical basis. We shall return to one of these prior results, dealing with the rate of adsorption on a plane,[1] in connection with eq 16.

In a recent paper,[2] one of us has shown that by using the simple method of reflections and superpositions a physically meaningful general expression for the kinetics of diffusion-controlled adsorption could be obtained for any shape for which the law of diffusion to a sink was known. We now present an analogous expression for the kinetics of concentration changes in the solution as adsorption proceeds. For the special case of an ideal adsorption isotherm, explicit solutions are also presented for both adsorption and concentration kinetics for the plane and for the sphere in a quiescent liquid. Future papers will be concerned with ideal adsorption when a stagnant layer is effective, which involves more complicated calculations, with Langmuirian adsorption, which requires numerical computations, and with asymptotic behavior, the analysis of which involves both of the above.

Concentration Changes

A solution of concentration C_∞, in equilibrium and bounded by a surface, may be considered as being the site of two opposite fluxes. One is transport of solute toward

---

* Address correspondence to the author at Research Consulting, 8327 La Jolla Senic Dr., La Jolla, CA 92037.

(1) Bakker, C. A. P.; Van Buytenen, P. M.; Beek, W. J. *Chem. Eng. Sci.* **1960**, *21*, 1039.

(2) Mysels, K. J. *J. Phys. Chem.* **1982**, *86*, 4648.

0022-3654/83/2087-3988$01.50/0